HHS Public Access

Author manuscript

Alzheimers Dement. Author manuscript; available in PMC 2023 August 04.

Published in final edited form as:

Alzheimers Dement. 2023 February ; 19(2): 518–531. doi:10.1002/alz.12675.

Predictive metabolic networks reveal sex and *APOE* genotype-specific metabolic signatures and drivers for precision medicine in Alzheimer Disease

Rui Chang[1,2,*,x,#], **Eugenia Trushina**[3,4,*,x], **Kuixi Zhu**[1,2,*], **Syed Shujaat Ali Zaidi**[1,2], **Branden M. Lau**[5], **Alexandra Kueider-Paisley**[6], **Sara Moein**[2,14], **Qianying He**[7], **Melissa L. Alamprese**[2], **Barbora Vagnerova**[8], **Andrew Tang**[9], **Ramachandran Vijayan**[1], **Yanyun Liu**[1], **Andrew J. Saykin**[10], **Roberta D. Brinton**[1,2,11,x], **Rima Kaddurah-Daouk**[6,12,13,x], **Alzheimer's Disease Neuroimaging Initiative Alzheimer's Disease Metabolomics Consortium**[†]

[1]Department of Neurology, University of Arizona, Tucson, AZ, USA

[2]The Center for Innovation in Brain Science, University of Arizona, Tucson, AZ, USA

[3]Department of Neurology, Mayo Clinic, Rochester, MN, USA

[4]Department of Molecular Pharmacology and Experimental Therapeutics, Mayo Clinic, Rochester, MN, USA

[5]Arizona Research Labs, Genetics Core, University of Arizona, Tucson, AZ, USA

[6]Department of Psychiatry and Behavioral Sciences, Duke University, Durham, NC, USA.

[7]Department of Biosystems Engineering, University of Arizona, Tucson, AZ, USA.

[8]Department of Pharmacology, College of Medicine, University of Arizona, Tucson, AZ, USA.

[9]Department of Neuroscience, University of Arizona, Tucson, AZ, USA

[10]Department of Radiology and Imaging Sciences and the Indiana Alzheimer Disease Center, Indiana University School of Medicine, Indianapolis, IN, USA

[11]Department of Pharmacology, College of Medicine, University of Arizona, Tucson, AZ, USA

[12]Duke Institute of Brain Sciences, Duke University, Durham, NC, USA

[13]Department of Medicine, Duke University, Durham, NC, USA

[14]Department of Pathology and Laboratory Medicine, Weill Cornell Medicine, New York, NY, USA

[#]corresponding author: ruichang@email.arizona.edu, Rui Chang, PhD, 1230 N Cherry Ave, PO Box 210242, Tucson, AZ. 85721-0242.

† Metabolomics data was generated by the Alzheimer Disease Metabolomics Consortium (https://sites.duke.edu/adnimetab/). Data used in preparation of this article were obtained from the Alzheimer's Disease Neuroimaging Initiative (ADNI) database (adni.loni.usc.edu). As such, the investigators within the ADNI contributed to the design and implementation of ADNI and/or provided data but did not participate in analysis or writing of this report. A complete listing of ADNI investigators can be found at: http://adni.loni.usc.edu/wp-content/uploads/how_to_apply/ADNI_Acknowledgement_List.pdf

[*]Tthese authors equally contributed to the manuscript

[x] co-senior authors

Competing interest statement

The other authors declare no competing interests.

Abstract

INTRODUCTION: LOAD is a complex neurodegenerative disease characterized by multiple progressive stages, glucose metabolic dysregulation, AD pathology, and inexorable cognitive decline. Discovery of metabolic profiles unique to sex, APOE-genotype and stage of disease progression could provide critical insights for personalized LOAD medicine.

METHODS: Sex- and *APOE*-specific metabolic networks were constructed based on changes in 127 metabolites of 656 serum samples from the ADNI cohort.

RESULTS: Application of advanced analytical platform identified metabolic drivers and signatures clustered with sex and/or *APOE*ε4, establishing patient-specific biomarkers predictive of disease state that significantly associated with cognitive function. Presence of the *APOE*ε4 shifts metabolic signatures to a phosphatidylcholine-focused profile overriding sex-specific differences in serum metabolites of AD patients.

DISCUSSION: These findings provide an initial but critical step in developing a diagnostic platform for personalized medicine by integrating metabolomic profiling and cognitive assessments to identify targeted precision therapeutics for AD patient subgroups through computational network modeling.

Keywords

Late-onset Alzheimer's disease; computational systems biology; metabolic network; metabolomics; ADNI; *APOE* ε4; sex-specific metabolic changes; metabolic biomarkers; precision medicine

1 BACKGROUND

Alzheimer's disease (AD) is a progressive neurodegenerative disorder without a cure. Recent clinical trial failures targeting β-amyloid (Aβ) or hyperphosphorylated tau protein (p-tau) underscore the importance of understanding disease-driving mechanisms. The primary risk factors of late-onset AD (LOAD), the predominant form, include age, female sex, and the presence of the *APOE*ε4 allele [1, 2]. LOAD is a multifactorial disorder with perturbations in glucose and insulin signaling, energy and lipid homeostasis, mitochondrial function, oxidative stress, inflammation, and neurotransmission [3, 4]. Recent progress in dissecting sex-specific mechanisms of AD has become possible through the implementation of systems-level approaches and availability of clinically characterized samples including ADNI cohort tissue and biofluids samples from AD patients and cognitively normal individuals enabling large-scale multi-omics studies. Metabolomics is the newest omics that measures thousands of metabolites reflecting alterations in genetic, transcriptomic, proteomic profiles, and influences from the environment [5, 6]. A large number of studies using metabolomcis and lipidomics platforms has provided new biochemical insights about disease mechanisms, early changes in disease and provided support that peripheral metabolic changes inform about central changes and ATN markers of disease [7–20].

We recently conducted stratified linear regression analyses of serum metabolites from 1517 ADNI participants to determine the association of metabolic signatures with disease

diagnosis (Dx) and A-T-N biomarkers (CSF $A\beta_{1-42}$ (A); CSF p-tau (T); FDG-PET (N)) [14] . Changes in metabolites associated with the Dx or A-T-N were influenced by sex and *APOE* and related to altered energy homeostasis [14]. We applied a recently developed computational predictive network model [21–24] to construct sex- and *APOE*-specific metabolic networks of CN and LOAD patients from the ADNI cohort in respect to sex and genotype and to clinical diagnosis cognitive parameters. We confirmed previous findings, demonstrated that metabolic panels associate with cognitive assessment, and identified metabolic drivers of LOAD. These findings further support the application of blood-based metabolomics as a precision medicine tool for disease stage profiling, prognosis, and identification of novel therapeutic targets.

2 METHODS

2.1 Participants

Figure 1 and Table 1 summarize information on ADNI participants utilized in this study.

2.2 Metabolomics data acquisition, normalization, and covariate adjustment

Metabolomics data normalization followed a six-step procedure [11] (Figure 1B, Online Method-1). Final 127 metabolites are listed in Table S1, and the final 362 CN and 294 AD samples were stratified into eight groups based on sex and *APOE* genotype (Table S2).

2.3 Predictive network Modeling

For each patient group, metabolites of AD and CN subjects were integrated with Dx into the predictive network modeling pipeline [22–25]. The network model consists of metabolites and Dx as nodes and causal interactions between them (Figure 2, Online Method-2).

2.4 Empirical non-parametric bootstrap and consensus network analysis

For each patient group, the 95% confidence interval (CI) of each edge was evaluated with the empirical bootstrap method (Online Method-3). To derive the patient-specific consensus metabolic networks, we included top 10% of edges with 95% confidence per patient group (Table S3). The metabolic signature was extracted as the 3-step upstream subnetwork of Dx in the patient-specific network (Table S4).

2.5 Evaluation of heterogeneity of key drivers

The heterogeneity of key drivers was evaluated by calculating the significance of robustness and confidence of patient-specific key driver in each patient group (Table S5, Online Method-4).

2.6 Differential expression (DE) analysis

Following covariate adjustment, metabolites were subjected to t-test using Limma R package [26] between AD and CN samples in each group (Figure 4, S1, Table S6).

2.7 Machine learning model and feature selection

To derive biomarker panel for each patient group, we employed a two-step machine learning procedure consisting of quantifying the feature importance in the first step followed by training elasticnet and XGBoost models to select a subset of features from input features (Online Method-5). To evaluate the prediction accuracy of every patient-specific panel, we performed 5-fold cross-validation in each group and repeated 100 times. The prediction performance was evaluated by calculating the averaged area under the curve (AUC).

2.8 Biomarker association with clinical features

For each biomarker panel, we extracted principal components that explained >90% of the variance in data. The response variables (clinical cognitive test scores) were regressed on these principal components, and ANOVA with F-statistics were used to calculate the fitness of regression. Multiple testing was adjusted by calculating the FDR value and significance reported based on FDR<0.05 (Table S8).

3 RESULTS

3.1 Sex- and *APOE*-specific consensus metabolic networks identify distinct metabolic signatures and drivers of LOAD

The analytical pipeline utilized in the study is presented in Figure 1. Consensus networks provide metabolic signatures defined as subnetworks containing metabolites within 3-steps upstream of Dx node. Metabolic key drivers are the immediate (1-step) metabolite(s) upstream of Dx node in each network (Figure 2, Table S4). To investigate the common metabolic signature of LOAD, we first built a background network by using 656 AD and CN samples without patient stratification (Figure 2A). This network identified changes in six phosphatidylcholines (PCs) with PC aa C36:6 as an immediate upstream driver regardless of sex or *APOE* genotype (Table S4A). The DE analysis confirmed significant changes in thirteen PCs, three sphingomyelins (SMs), four acylcarnitines and citrulline (Table S6A).

To reveal sex-specific differences, we built consensus metabolic networks using residuals of 161 AD and 177 CN males and 133 AD and 185 CN females. The male consensus network (Figure 2B) identified changes in amino acids valine, isoleucine, lysine and tryptophan mediated by alpha-amino adipic acid (alpha-AAA) (Table S4B). The DE analysis confirmed increased levels of three acylcarnitines and a decrease in sarcosine, two PCs and one sphingomyelin (SM) (Table S6B). Levels of valine, a metabolite directly connected to alpha-AAA, were decreased by more than 7-fold ($P = 0.13$, Table S6B). The female consensus network (Figure 2C) was dominated by reduced levels of four PCs, one SM and tryptophan, and an increase in creatinine (Table S6C). These data suggest that AD was mainly associated with changes in amino acids in males, and PCs and tryptophan in females.

To define *APOE*-specific metabolic signatures, we built consensus networks using residuals of 193 AD and 101 CN *APOE*ε4+ and 101 AD and 261 CN *APOE*ε4-. The *APOE*ε4+ consensus network (Figure 2D) revealed a homogeneous signature of six PCs mediated by PC aa C34:4 (Table S4D). The DE analysis confirmed significant changes in four PCs (Table S6D). The *APOE*ε4- consensus network (Figure 2E) identified a mixed signature of valine,

isoleucine, alpha-AAA, tryptophan, creatinine, lysine, proline, two acylcarnitines, and 26 PCs mediated by PC aa C38:0 and alpha-AAA (Table S4E). The DE analysis confirmed a significant decrease in nine PCs, four SMs, sarcosine, lysine, and valine, and an increase in creatinine and citrulline, three acylcarnitines and a pro-inflammatory agent symmetric dimethylarginine (Table S6E). These results demonstrate that *APOE* ε4 allele specifically affects the metabolism of PCs.

Next, we built male *APOE*ε4+, male *APOE*ε4-, female *APOE*ε4+, and female *APOE*ε4- consensus networks by using 107/47, 54/130, 86/54 and 47/131 AD/CN residuals, respectively (Figure 2F–2I). The male *APOE*ε4+ network (Figure 2F) identified a homogeneous signature of 22 PCs and five SMs (Table S4F). The DE analysis revealed significant decrease in taurine and carnitine C7-DC, and an increase in asparagine and lyso-PC a C18:0. While not statistically significant, levels of alanine and lysine decreased by more than 8- and 3-fold, respectively, whereas levels of glycine, threonine, ornithine, and glutamate increased by more than 20-, 5-, 3- and 3-fold, respectively. The male *APOE*ε4- consensus network (Figure 2G) identified changes in ten acylcarnitines, five amino acids and three lyso-PCs (Table S4G). A decrease in sarcosine and two PCs and an increase in six acylcarnitines were significant in LOAD compared to CN. While not significant, levels of branched chain amino acids (BCAA) valine and isoleucine and amino acids lysine, glutamate, isoleucine, and arginine were decreased while levels of citrulline, glycine, creatinine, alanine and taurine were increased from 2 to 13-fold (Table S4G).

The female *APOE*ε4+ consensus network (Figure 2H) identified a PC-dominant signature (Table S4H). DE analysis revealed significantly decreased PCs and essential amino acid L-tryptophan. Levels of alanine and lysine decreased by more than 18- and 6-fold, respectively, whereas glycine, proline, and arginine increased by more than 6-, 4- and 4-fold, respectively, though not statistically significant. In female *APOE*ε4- carriers, the consensus network discovered a mixed signature of eight SMs and three PCs (Figure 2I, Table S4I). The DE analysis revealed significantly decreased four PCs and amino acids L-tryptophan, taurine, lysine, as well as significantly increased citrulline and creatine. Summary for each group is presented in Table 2.

3.3 Heterogeneity in patient group-specific metabolic key drivers

The consensus network analysis revealed distinct patterns of homogeneity/heterogeneity in the metabolic signatures within each patient group. While this network captures the most robust signal relative to all individuals in each patient group, it doesn't address the endogenous metabolic heterogeneity associated with different subpopulations within the same group. To further investigate inherent metabolic heterogeneity, we calculated the significance (FDR adjusted) of robustness and confidence for every key driver in each group (Table S5). Robustness of metabolic drivers was determined based on their connection to Dx with positive 95% CI, significant robustness, and confidence. Despite multiple potential metabolic drivers identified in each subpopulation group, the following metabolites robustly connected to Dx: males: alpha-AAA; females: PC aa C36:6 and tryptophan; *APOE*ε4+: PC aa C34:4; *APOE*ε4-: PC aa C38:0, alpha-AAA, and serotonin; male *APOE*ε4+: PC ae C36:3

and PC aa C40:2; male *APOE*ε4-: C6 and sarcosine; female *APOE*ε4+: PC aa C34:4, PC ae C36:4 and L-tryptophan; and female *APOE*ε4-: SM C26:0 (Figure 3, Table 2, Table S5).

3.4 Metabolic network cross-validation using sex- and *APOE*-specific biomarker panel

To validate metabolic networks and key drivers, we trained an ensemble of machine learning models to select a subset of metabolites based on the network model and drivers with changes significantly associated with the disease state in each patient group. The prediction performance was evaluated with averaged AUC by cross-validation in the ADNI data (Figure 5). In each patient group, we trained different models and compared AUCs of each model with eight sets of input features. Set 1: all 127 metabolites; Set 2: significant DE metabolites; Set 3: network-derived metabolites; Set 4: combination of all 127 metabolites plus age, education, BMI; Set 5: significant DE metabolites plus demographics; Set 6: network-derived metabolites plus age, education length, BMI; Set 7: network-derived metabolites plus significant DE metabolites; Set 8: network-derived metabolites plus significant DE metabolites and age, education, BMI. The network-derived metabolites were extracted from the neighbor (within 3-step undirected) subnetwork of the Dx node in respectful networks.

We found that the prediction accuracy (AUC) of the network-derived metabolites (Set 3, Figure 5 green line) robustly and significantly outperformed those predicted by using all metabolites in the data (Set 1, Figure 5 black line) and only significant (P<0.05) DE metabolites derived from the linear regression model (Set 2, Figure 5 purple line) across all patient groups. Adding patient demographics to Sets 1 and 3 greatly improved individual prediction accuracy. However, the same pattern was observed in their relative accuracy, i.e., the AUC produced by the network-derived metabolite with patient demographics (Set 6, Figure 5 orange line) consistently outperformed the accuracy predicted by adding demographics to either all metabolites in the data (Set 4, Figure 5 pink line) or only significant (P<0.05) DE metabolites (Set 5, Figure 5 blue line) across all patient groups. When significant DE metabolites were added to the combination of network-derived features with patient demographics (Set 8, Figure 5 red line), a marginal improvement in AUC was observed in all *APOE*ε4-, female *APO*ε4+ and female *APOE*ε4- groups, with a slight decrease in AUC was observed in males, male *APOE*ε4+, male *APOE*ε4-, suggesting that significant DE metabolites derived from linear regression added no further power in prediction of Dx given the network structure and patient demographics. Data suggest that the metabolic network-derived features with or without age, BMI, and education significantly improved the prediction accuracy compared to the other feature sets, DE metabolites and all 127 metabolites in the data, across all patient groups. These data indicate that the predictive network model utilized in this study is more sensitive than traditional regression method in detecting weaker relations of metabolic changes with disease state in sex- and *APOE*-specific patient groups. The best performing feature set with or without demographics, respectively, was selected for each group as the biomarker panel (Table S7).

3.5 Blood-based metabolic biomarker panels associate with cognitive decline

To evaluate the association of selected biomarker panels with clinical cognitive assessment (diagnosis, ADAS-Cog score, memory, and executive function), we calculated the eigen

expression to recapitulate the primary variance component (the first principal component) for each panel and fitted a linear regression model between the eigen expression of the 1st principal component and cognitive measures. Significance of association is shown in Figure 5I (Table S8). Network-derived biomarker panels for each patient group with or without demographics were all significantly associated with the Dx. Of 16 panels (Table S7, two selected panels per group times 8 patient groups), 13 and 15 panels were significantly associated with memory (ADNI_MEM) and the overall cognition (ADAS-Cog Total Score), respectively. Of 16 panels, 10 were significantly associated with the executive function composite score (ADNI_EF). Two biomarker panels approached statistical significance with the executive function composite score: network-derived features with demographics for male *APOE*ε4+ (FDR=0.0667) and network-derived features without demographic for female *APOE*ε4+ (FDR=0.0678). Two biomarker panels approached statistical significance with overall cognition score: network-derived features with (FDR=0.0655) and without (FDR=0.0667) demographics. These results indicate that patient-specific metabolic networks and network-derived biomarker panels are associated with clinical cognitive assessment.

4 Discussion

Using advanced computational method, we demonstrated that LOAD is associated with metabolomic profiles defined by sex and *APOE* genotype. Based on patient group-specific network models, we identified key drivers, differentially produced metabolites and metabolic signatures of the disease. Unstratified analyses identified changes in lipid homeostasis, with carnitines, PCs and SMs as most affected metabolites that differentiated AD from CN. Further stratification by sex revealed that metabolic changes in AD males were associated with amino acids while lipids remained predominantly affected in females. Stratification by sex and *APOE* did not affect lipid-dominant metabolic signatures in females while in *APOE*ε4+ males, metabolic drivers and signatures changed from amino acids, especially BCAAs, to lipids comparable to *APOE*ε4+ females. In *APOE*ε4- males and females, metabolic changes were more diverse compared to *APOE*ε4+ and included lipids and amino acids. The identified metabolic alterations are consistent with previous reports where changes in blood levels of PCs, SMs, acylcarnitines, ceramides, and amino acids differentiated MCI and AD from CN [11, 14, 18, 19, 27–30].

In addition to replicating sex-specific differences in serum metabolites associated with AD [14], our analyses also generated multiple novel and important findings by identifying metabolic signatures and key drivers in patient groups stratified by the intersection of sex and *APOE* genotype, which has not been previously reported. We demonstrate that i) previously observed amino acid-centered metabolic signatures and drivers in AD males are true for males without *APOE*ε4; (ii) metabolic signatures and drivers for *APOE*ε4+ males shifted from amino acids to lipids (PCs and SMs) similar to changes observed in *APOE*ε4+ females. This important finding highlights the ability of *APOE*ε4 genotype to signifinatly influence metabolic changes overriding sex-specific differences observed in serum metabolites in AD males and females. (iii) The metabolic shift is more subtle between *APOE*ε4+ and *APOE*ε4- females, which is confined to different lipid species, i.e., the shift from a SM-dominant metabolic signatures and drivers in *APOE*ε4- to a PC-dominant signatures and drivers in *APOE*ε4+. Overall, our novel findings indicate that *APOE*ε4

genotype drives metabolic signature to a phosphatidylcholine-focused profile regardless of the patient sex.

The replicative validity and novelty of our findings emphasizes the importance of these metabolic pathways for AD. We identified changes in numerous individual lipids, including PCs and lysoPCs, as key drivers or components of metabolic signatures associated with cognition. PCs and SMs are integral constituents of the plasma membrane. The reduced PC levels observed in AD may reflect abnormal membrane functions including synaptic transmission and processing of the amyloid precursor protein contributing to Aβ production [31]. Furthermore, alterations in PCs may contribute to increased inflammation, one of the underlying mechanisms of LOAD [32, 33]. The panel of PCs and carnitines predicted the conversion from CN to AD/aMCI with sensitivity and specificity of 90% [27, 34] yielding improvements to previous reports where stratification was not used [35–37]. L-Carnitine and acylcarnitines play an essential role in energy metabolism transporting activated long-chain fatty acids into mitochondria for β-oxidation. They also mediate the metabolism of BCAAs, neuromodulation, antioxidant and anti-apoptotic functions in the brain [38, 39]. Consistent with our findings, changes in multiple carnitines (e.g., C12, C12:1, C14:1 and C8) contributed to discriminating AD from CN [40–42]. A recent study with the same metabolomics data conducted in both ante-mortem blood and post-mortem brain samples in two community-based longitudinal aging and dementia cohorts reported that decanoylcarnitine C10, pimelylcarnitine C7-DC, and tetradecadienylcarnitine C14:2 significantly predicted a lower AD risk after a 4.5-year follow-up, independent of age, sex, and education [34]. However, the most important changes in carnitines and amino acids detected in AD patients associate with sex-specific dysregulation of energy metabolism [2, 43].

Altered glucose uptake in the brain detected using FDG-PET occurs decades before onset of AD symptoms, suggesting that metabolic deficits are an upstream event specific to LOAD [43, 44]. Thus, changes in carnitines, fatty acids and amino acids, BCAA in particular, may indicate differential compensatory mechanisms for alternative energy substrates in AD males and females [45, 46]. High levels of carnitines may indicate a buildup of fatty acids, suggesting increased energy demands coupled with impaired energy production via mitochondrial β-oxidation [46]. Male-specific metabolic signatures identified herein included alpha-AAA and BCAA valine and isoleucine. BCAAs are important energy carrying molecules associated with cognitive decline and brain atrophy in AD [47]. Changes in their levels could indicate a switch to increased energy consumption via degradation of amino acids. The biogenic amine alpha-AAA is a degradation product of lysine and is involved in mechanisms of neurotransmission [48, 49]. Higher levels of serum alpha-AAA are associated with decreased cognitive function [5]. Consistent with previous observations, we detected positive associations of AD cognitive function with multiple amino acids, including tryptophan, citrulline, sarcosine, aspartic acid, and taurine [5, 11, 14, 18–20].

Our study has several limitations. First, the AbsoluteIDQ-p180 system is a targeted metabolomic platform with limited set of metabolites, including amino acids (21), biogenic amines (21), hexose (1), acylcarnitines (40), lysophosphatidylcholines (14), phosphatidylcholines (76), and sphingolipids (15). Utilization of this platform enabled

a direct comparison of the results reported herein, generated using advanced analytical computational analysis, to previously generated findings using the same platform[14]. Our novel computational systems biology approach enabled findings that strongly support utility of the targeted metabolomic biomarker translational approach for individualized medicine. Future large-scale metabolomics analyses could provide greater detail that support the metabolic pathways reported herein while also identifying additional pathways. From a translational perspective the replication of affected pathways using the targeted metabolomic platform coupled with a novel systems biology computational approach enabled identification of sex, APOE genotype and AD stage specific phenotypes. These findings provide the foundation for personalized therapeutic interventions and simultaneously a biomarker strategy to determine target engagement and therapeutic efficacy. Second, the metabolic data are inherently susceptible to environmental influences and personal factors. Such variability is further amplified in stratified analyses like ours, where although starting with thousands of patients, stratification reduces group size resulting in smaller detection power. Thus, most of significant DE didn't survive multiple-testing correction. Therefore, potentially important findings could be missed by using conventional analytical methods such as DE and linear regression. We addressed this problem by utilizing a more sensitive network model than conventional methods. Our network model exploited the conditional independence derived from the robust covariance structure to overcome the relatively small effect-size in metabolic data due to random noise and small detection power due to reduced number of patients by stratification, which is not well handled by linear regression and correlation-based methods[14]. Herein, we demonstrated that our network approach is more robust and sensitive for detecting true associations over conventional methods. This may explain why previous studies have not discovered that *APOEε4* status overrides sex-specific difference in serum AD metabolites though a similar effect was observed in a recent study with humanized APOE mice [30]. Although our network approach to some extent can mathematically alleviate the issue of low detection power, the number of subjects in each group was relatively small and studies in larger longitudinal cohorts are warranted to confirm these results. Our Alzheimer Disease Metabolomics Consortium (ADMC) is conducting comprehensive metabolic profiling across metabolomic platforms to provide broad biochemical coverage of the metabolome to map metabolic failures across trajectory of disease.

In summary, we provide a compelling systems biology analytical platform for metabolomics data analysis. We identified sex- and *APOE*-specific metabolic signatures associated with clinical diagnosis and cognitive assessment and key metabolic drivers that could be evaluated as therapeutic targets with a potential to shift the trajectory of the disease. The metabolic signatures and key drivers demonstrated clear metabolic differences in sex and *APOE* genotype and highlighted the potential of *APOE*ε4 genotype overriding sex-difference in human serum metabolic associated with AD. In addition, we identified serum metabolic panels significantly associated with clinical diagnosis and cognitive assessment in each patient subgroup. This is the first study to establish patient-specific serum metabolic biomarkers predictive of disease diagnosis that significantly associated with clinical cognitive assessment for individual groups of patients stratified by sex and *APOE* genotype (Figure 5I, Table S9). Based on the biomarker panel of network-derived

metabolites and demographic features, we identified that education attainment and BMI are two most common biomarkers shared by 5 out of 8 patient groups, followed by tryptophan (4 out of 8), a set of PCs (PC aa C42:6, PC ae C36:5, PC ae C40:2, PC ae C42:5, PC ae C36:0) and age (3 out of 8). Interestingly, we identified valine, creatinine, lysine, C16, SM C26:1, lysoPC a C16:1, lysoPC a C18:0, lysoPC a C18:2, lysoPC a C20:3, PC aa C32:1, PC ae C38:5, PC ae C42:3 as unique markers for males; alpha-AAA and sarcosine as specific markers for *APOE*ε4- males; C14:1-OH, PC aa C40:3, PC ae C30:0, SM (OH) C22:1 and taurine as unique markers for *APOE*ε4+ males; PC aa C34:4 as a specific marker for *APOE*ε4- females; and PC aa C38:0 as a specific marker for *APOE*ε4+ females.

Our study provides an initial but critical step towards developing personalized and precision medicine for AD and an operational strategy to achieve that goal, which integrates clinical cognitive assessment, metabolomic profiling, and computational network model to identify targeted therapeutic strategies for subsets of patients.

Supplementary Material

Refer to Web version on PubMed Central for supplementary material.

Acknowledgement

Data collection and sharing for this project was funded by the Alzheimer's Disease Neuroimaging Initiative (ADNI) (National Institutes of Health Grant U01 AG024904) and DOD ADNI (Department of Defense award number W81XWH-12–2-0012). ADNI is funded by the National Institute on Aging, the National Institute of Biomedical Imaging and Bioengineering, and through generous contributions from the following: AbbVie, Alzheimer's Association; Alzheimer's Drug Discovery Foundation; Araclon Biotech; BioClinica, Inc.; Biogen; Bristol-Myers Squibb Company; CereSpir, Inc.; Cogstate; Eisai Inc.; Elan Pharmaceuticals, Inc.; Eli Lilly and Company; EuroImmun; F. Hoffmann-La Roche Ltd and its affiliated company Genentech, Inc.; Fujirebio; GE Healthcare; IXICO Ltd.; Janssen Alzheimer Immunotherapy Research & Development, LLC.; Johnson & Johnson Pharmaceutical Research & Development LLC.; Lumosity; Lundbeck; Merck & Co., Inc.; Meso Scale Diagnostics, LLC.; NeuroRx Research; Neurotrack Technologies; Novartis Pharmaceuticals Corporation; Pfizer Inc.; Piramal Imaging; Servier; Takeda Pharmaceutical Company; and Transition Therapeutics. The Canadian Institutes of Health Research is providing funds to support ADNI clinical sites in Canada. Private sector contributions are facilitated by the Foundation for the National Institutes of Health (www.fnih.org). The grantee organization is the Northern California Institute for Research and Education, and the study is coordinated by the Alzheimer's Therapeutic Research Institute at the University of Southern California. ADNI data are disseminated by the Laboratory for Neuro Imaging at the University of Southern California.

This research was supported by grants from the National Institutes of Health and partnership with Alzheimer's Disease Metabolomics Consortium (ADMC) [grant numbers RF1AG057457 and R56AG062620 to R.C., RF1AG059093 to R.B., R.C. and R.K., R01AG057931 to R.B. and R.C, RF1AG55549, R01NS107265 and R01AG062135 to E.T.]. **The results published here are in whole or in part based on data obtained from the AD Knowledge Portal (** https://adknowledgeportal.org). Metabolomics data is provided by the Alzheimer's Disease Metabolomics Consortium (ADMC) and funded wholly or in part by the following grants and supplements thereto: NIA R01AG046171, RF1AG051550, RF1AG057452, R01AG059093, RF1AG058942, U01AG061359, U19AG063744 and FNIH: #DAOU16AMPA awarded to Dr. Kaddurah-Daouk at Duke University in partnership with a large number of academic institutions. As such, the investigators within the ADMC, not listed specifically in this publication's author's list, provided data along with its pre-processing and prepared it for analysis, but did not participate in analysis or writing of this manuscript. A complete listing of ADMC investigators can be found at: https://sites.duke.edu/adnimetab/team/.

We thank Drs. Matthias Arnold (MA) and Gabi Kasternmuller (GK) from Institute of Bioinformatics and Systems Biology, Helmholtz Zentrum München for their discussions. Additionally, MA, R.K-D, and GK are supported by NIA grants RF1 AG058942 and R01 AG057452. MA and GK are also supported by funding from Qatar National Research Fund NPRP8-061-3-011. Its contents are solely the responsibility of the authors and do not necessarily represent the official view of the NIH. The funders had no role in study design, data collection and analysis, decision to publish, or preparation of the manuscript.

R.C. is the founder of INTelico Therapeutics LLC and co-founder of PATH Biotech LLC. RKD in an inventor on a series of patents on use of metabolomics for the diagnosis and treatment of CNS and ther diseases and holds founding equity in Metabolon Inc., Chymia LLC and PsyProtix. This study was not supported by any of above companies.

List of Abbreviations

APOE	apolipoprotein E
ADNI	Alzheimer's Disease Neuroimaging Initiative
ADMC	Alzheimer Disease Metabolomics Consortium
LOAD	Late-onset Alzheimer's disease
APOEε4	ε4 allele of the Apolipoprotein E (APOE)
AD	Alzheimer's Disease
Aβ	amyloid beta
CN	cognitively normal
CSF	cerebrospinal fluid
MCI	mild cognitive impairment
Aβ1–42	amyloid beta peptide 1–42
p-tau	hyperphosphorylated-tau protein
FDG-PET	fluorodeoxyglucose-positron emission tomography
Dx	disease diagnosis
BMI	body mass index
BN	Bayesian network
CI	confidence interval
XGBoost	eXtreme Gradient Boosting
AUC	area under curve
ANOVA	analysis of variance
FDR	false discovery rate
PC	phosphatidylcholine
DE	Differential Expression
SM	sphingomyelin
alpha-AAA	alpha-amino adipic acid

APOEε4-	*APOEε4* negative/non-carrier
APOEε4+	*APOEε4* positive/carrier
C7-DC	Pimelylcarnitine
lyso-PC	Lysophosphatidylcholine
BCAA	branched chain amino acid
ADAS-Cog	The Alzheimer's Disease Assessment Scale–Cognitive Subscale
ADNI_MEM	Alzheimer's Disease Neuroimaging Initiative Memory Test Score
ADNI_EF	Alzheimer's Disease Neuroimaging Initiative Executive Function Test Score
aMCI	amnestic mild cognitive impairment

References

1. Jansen IE, et al. , Genome-wide meta-analysis identifies new loci and functional pathways influencing Alzheimer's disease risk. Nat Genet, 2019. 51(3): p. 404–413. [PubMed: 30617256]
2. Guo L, et al. , Sex Differences in Alzheimer's Disease: Insights From the Multiomics Landscape. Biol Psychiatry, 2021.
3. Talwar P, et al. , Dissecting Complex and Multifactorial Nature of Alzheimer's Disease Pathogenesis: a Clinical, Genomic, and Systems Biology Perspective. Mol Neurobiol, 2016. 53(7): p. 4833–64. [PubMed: 26351077]
4. Zhang B, et al. , Integrated systems approach identifies genetic nodes and networks in late-onset Alzheimer's disease. Cell, 2013. 153(3): p. 707–20. [PubMed: 23622250]
5. Wilkins JM and Trushina E, Application of Metabolomics in Alzheimer's Disease. Front Neurol, 2017. 8: p. 719. [PubMed: 29375465]
6. Niedzwiecki MM, et al. , High-resolution metabolomic profiling of Alzheimer's disease in plasma. Ann Clin Transl Neurol, 2020. 7(1): p. 36–45. [PubMed: 31828981]
7. Trushina E, et al. , Identification of altered metabolic pathways in plasma and CSF in mild cognitive impairment and Alzheimer's disease using metabolomics. PLoS One, 2013. 8(5): p. e63644.
8. Han X, et al. , Metabolomics in early Alzheimer's disease: identification of altered plasma sphingolipidome using shotgun lipidomics. PLoS One, 2011. 6(7): p. e21643.
9. Kaddurah-Daouk R, et al. , Metabolomic changes in autopsy-confirmed Alzheimer's disease. Alzheimers Dement, 2011. 7(3): p. 309–17. [PubMed: 21075060]
10. Kaddurah-Daouk R, et al. , Alterations in metabolic pathways and networks in Alzheimer's disease. Transl Psychiatry, 2013. 3: p. e244. [PubMed: 23571809]
11. Toledo JB, et al. , Metabolic network failures in Alzheimer's disease: A biochemical road map. Alzheimers Dement, 2017. 13(9): p. 965–984. [PubMed: 28341160]
12. Nho K, et al. , Altered bile acid profile in mild cognitive impairment and Alzheimer's disease: Relationship to neuroimaging and CSF biomarkers. Alzheimers Dement, 2019. 15(2): p. 232–244. [PubMed: 30337152]
13. Nho K, et al. , Association of Altered Liver Enzymes With Alzheimer Disease Diagnosis, Cognition, Neuroimaging Measures, and Cerebrospinal Fluid Biomarkers. JAMA Netw Open, 2019. 2(7): p. e197978.
14. Arnold M, et al. , Sex and APOE epsilon4 genotype modify the Alzheimer's disease serum metabolome. Nat Commun, 2020. 11(1): p. 1148. [PubMed: 32123170]
15. Bernath MM, et al. , Serum triglycerides in Alzheimer disease: Relation to neuroimaging and CSF biomarkers. Neurology, 2020. 94(20): p. e2088–e2098. [PubMed: 32358220]

16. Huynh K, et al. , Concordant peripheral lipidome signatures in two large clinical studies of Alzheimer's disease. Nat Commun, 2020. 11(1): p. 5698. [PubMed: 33173055]
17. Baloni P, et al. , Metabolic Network Analysis Reveals Altered Bile Acid Synthesis and Metabolism in Alzheimer's Disease. Cell Rep Med, 2020. 1(8): p. 100138.
18. Nho K, et al. , Serum metabolites associated with brain amyloid beta deposition, cognition and dementia progression. Brain Commun, 2021. 3(3): p. fcab139.
19. Horgusluoglu E, et al. , Integrative metabolomics-genomics approach reveals key metabolic pathways and regulators of Alzheimer's disease. Alzheimers Dement, 2021.
20. Batra R, et al. , The landscape of metabolic brain alterations in Alzheimer's disease. bioRxiv, 2021: p. 2021.11.15.468698.
21. Chang R and Schadt E, Patent US2019019864. SYSTEMS AND METHODS FOR PREDICTIVE NETWORK MODELING FOR COMPUTATIONAL SYSTEMS, BIOLOGY AND DRUG TARGET DISCOVERY 2019.
22. Petyuk VA, et al. , The human brainome: network analysis identifies HSPA2 as a novel Alzheimer's disease target. Brain, 2018. 141(9): p. 2721–2739. [PubMed: 30137212]
23. Carcamo-Orive I, et al. , Analysis of Transcriptional Variability in a Large Human iPSC Library Reveals Genetic and Non-genetic Determinants of Heterogeneity. Cell Stem Cell, 2017. 20(4): p. 518–532. [PubMed: 28017796]
24. Carcamo-Orive I, et al. , Predictive network modeling in human induced pluripotent stem cells identifies key driver genes for insulin responsiveness. PLoS Comput Biol, 2020. 16(12): p. e1008491.
25. Kruti Rajan Patel KZ, Marc Y.R. Henrion, Beckmann Noam D., Moein Sara, Alamprese Melissa L., Allen Mariet, Wang Xue, Chan Gail, Pertel Thomas, Nejad Parham, Reddy Joseph S., Carrasquillo Minerva M., Bennett David A, Ertekin-Taner Nilüfer, De Jager Philip L., Schadt# Eric E., Bradshaw# Elizabeth M., Chang# Rui, Single Cell-type Integrative Network Modeling Identified Novel Microglial-specific Targets for the Phagosome in Alzheimer's disease. bioRxiv, 2020.
26. Ritchie ME, et al. , limma powers differential expression analyses for RNA-sequencing and microarray studies. Nucleic Acids Res, 2015. 43(7): p. e47. [PubMed: 25605792]
27. Mapstone M, et al. , Plasma phospholipids identify antecedent memory impairment in older adults. Nat Med, 2014. 20(4): p. 415–8. [PubMed: 24608097]
28. Klavins K, et al. , The ratio of phosphatidylcholines to lysophosphatidylcholines in plasma differentiates healthy controls from patients with Alzheimer's disease and mild cognitive impairment. Alzheimers Dement (Amst), 2015. 1(3): p. 295–302. [PubMed: 26744734]
29. Oeckl P and Otto M, A Review on MS-Based Blood Biomarkers for Alzheimer's Disease. Neurol Ther, 2019. 8(Suppl 2): p. 113–127. [PubMed: 31833028]
30. Shang Y, et al. , Evidence in support of chromosomal sex influencing plasma based metabolome vs APOE genotype influencing brain metabolome profile in humanized APOE male and female mice. PLoS One, 2020. 15(1): p. e0225392.
31. Kosicek M and Hecimovic S, Phospholipids and Alzheimer's disease: alterations, mechanisms and potential biomarkers. Int J Mol Sci, 2013. 14(1): p. 1310–22. [PubMed: 23306153]
32. Che H, et al. , Comparative study of the effects of phosphatidylcholine rich in DHA and EPA on Alzheimer's disease and the possible mechanisms in CHO-APP/PS1 cells and SAMP8 mice. Food Funct, 2018. 9(1): p. 643–654. [PubMed: 29292421]
33. Hur JY, et al. , The innate immunity protein IFITM3 modulates gamma-secretase in Alzheimer's disease. Nature, 2020. 586(7831): p. 735–740. [PubMed: 32879487]
34. Huo Z, et al. , Brain and blood metabolome for Alzheimer's dementia: findings from a targeted metabolomics analysis. Neurobiol Aging, 2020. 86: p. 123–133. [PubMed: 31785839]
35. Casanova R, et al. , Blood metabolite markers of preclinical Alzheimer's disease in two longitudinally followed cohorts of older individuals. Alzheimers Dement, 2016. 12(7): p. 815–22. [PubMed: 26806385]
36. Li D, et al. , Plasma phospholipids and prevalence of mild cognitive impairment and/or dementia in the ARIC Neurocognitive Study (ARIC-NCS). Alzheimers Dement (Amst), 2016. 3: p. 73–82. [PubMed: 27408938]

37. Li D, et al. , Prospective associations of plasma phospholipids and mild cognitive impairment/dementia among African Americans in the ARIC Neurocognitive Study. Alzheimers Dement (Amst), 2017. 6: p. 1–10. [PubMed: 28054030]
38. Jones LL, McDonald DA, and Borum PR, Acylcarnitines: role in brain. Prog Lipid Res, 2010. 49(1): p. 61–75. [PubMed: 19720082]
39. Mihalik SJ, et al. , Increased levels of plasma acylcarnitines in obesity and type 2 diabetes and identification of a marker of glucolipotoxicity. Obesity (Silver Spring), 2010. 18(9): p. 1695–700. [PubMed: 20111019]
40. Ciavardelli D, et al. , Medium-chain plasma acylcarnitines, ketone levels, cognition, and gray matter volumes in healthy elderly, mildly cognitively impaired, or Alzheimer's disease subjects. Neurobiol Aging, 2016. 43: p. 1–12. [PubMed: 27255810]
41. Cristofano A, et al. , Serum Levels of Acyl-Carnitines along the Continuum from Normal to Alzheimer's Dementia. PLoS One, 2016. 11(5): p. e0155694.
42. Gonzalez-Dominguez R, et al. , Metabolomic profiling of serum in the progression of Alzheimer's disease by capillary electrophoresis-mass spectrometry. Electrophoresis, 2014. 35(23): p. 3321–30. [PubMed: 25136972]
43. Cunnane SC, et al. , Brain energy rescue: an emerging therapeutic concept for neurodegenerative disorders of ageing. Nat Rev Drug Discov, 2020. 19(9): p. 609–633. [PubMed: 32709961]
44. Mosconi L, Glucose metabolism in normal aging and Alzheimer's disease: Methodological and physiological considerations for PET studies. Clin Transl Imaging, 2013. 1(4).
45. Lynch CJ and Adams SH, Branched-chain amino acids in metabolic signalling and insulin resistance. Nat Rev Endocrinol, 2014. 10(12): p. 723–36. [PubMed: 25287287]
46. Sharma S and Black SM, Carnitine Homeostasis, Mitochondrial Function, and Cardiovascular Disease. Drug Discov Today Dis Mech, 2009. 6(1–4): p. e31–e39. [PubMed: 20648231]
47. Tynkkynen J, et al. , Association of branched-chain amino acids and other circulating metabolites with risk of incident dementia and Alzheimer's disease: A prospective study in eight cohorts. Alzheimers Dement, 2018. 14(6): p. 723–733. [PubMed: 29519576]
48. Chang YE, Lysine metabolism in the rat brain: the pipecolic acid-forming pathway. J Neurochem, 1978. 30(2): p. 347–54. [PubMed: 624941]
49. Guidetti P and Schwarcz R, Determination of alpha-aminoadipic acid in brain, peripheral tissues, and body fluids using GC/MS with negative chemical ionization. Brain Res Mol Brain Res, 2003. 118(1–2): p. 132–9. [PubMed: 14559362]

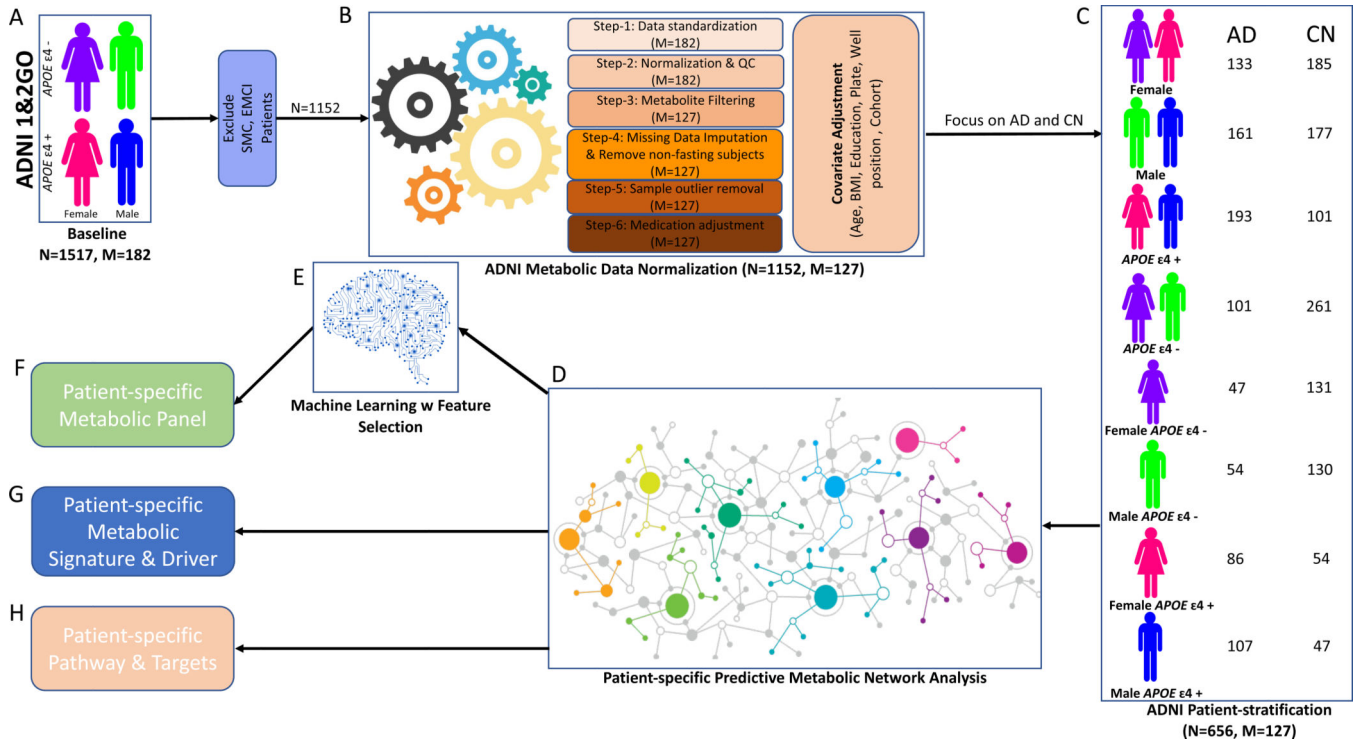

Figure 1. Analytical pipeline utilized in the study.

The analytical pipeline included 1152 samples from ADNI cohort. Patients with self-memory complain (SMC) and early mild cognitive impairment (EMCI) were removed leaving 1152 samples from AD, late mild cognitive impairment (LMCI) and CN (A). Data were normalized; the residuals were obtained after covariate adjustment (B). 362 CN and 294 AD samples were stratified into eight groups based on sex and *APOE* genotype (C). A predictive network model was built (D) to derive patient-specific metabolic signatures and drivers of progression from CN to AD in each group (G). The DE analysis identified significant changes in metabolites. Metabolic biomarker panels (F) were derived using machine learning models (E). Patient-specific pathways were identified based on metabolic signatures and drivers (H). N, the number of participants; M, the number of metabolites; ADNI, AD Neuroimaging Initiative; ADNI 1&2GO, phase 1 and phase 2/GO of ADNI; QC, quality control; AD, Alzheimer disease; CN, cognitive normal; BMI, body mass index.

Figure 2. Sex- and *APOE*-specific consensus predictive metabolic network

To build consensus causal predictive metabolic network, we subsampled 100 datasets and constructed 100 metabolic networks per patient group. The 95% confidence interval is calculated per edge. The consensus network models were used to identify the upstream metabolites and pathways associated with AD in background with all 656 AD and CN samples (A), males (B), females (C), *APOE*ε4+ (D), *APOE*ε4- (E), male *APOE*ε4+ (F), male *APOE*ε4- (G), female *APOE*ε4+ (H), female *APOE*ε4- (I). Dx, disease diagnosis. Red color indicates metabolites metabolite level is increased in AD comparing to CN; green color indicates metabolite level is decreased in AD comparing to CN. Significant DE metabolites are indicated with black circles.

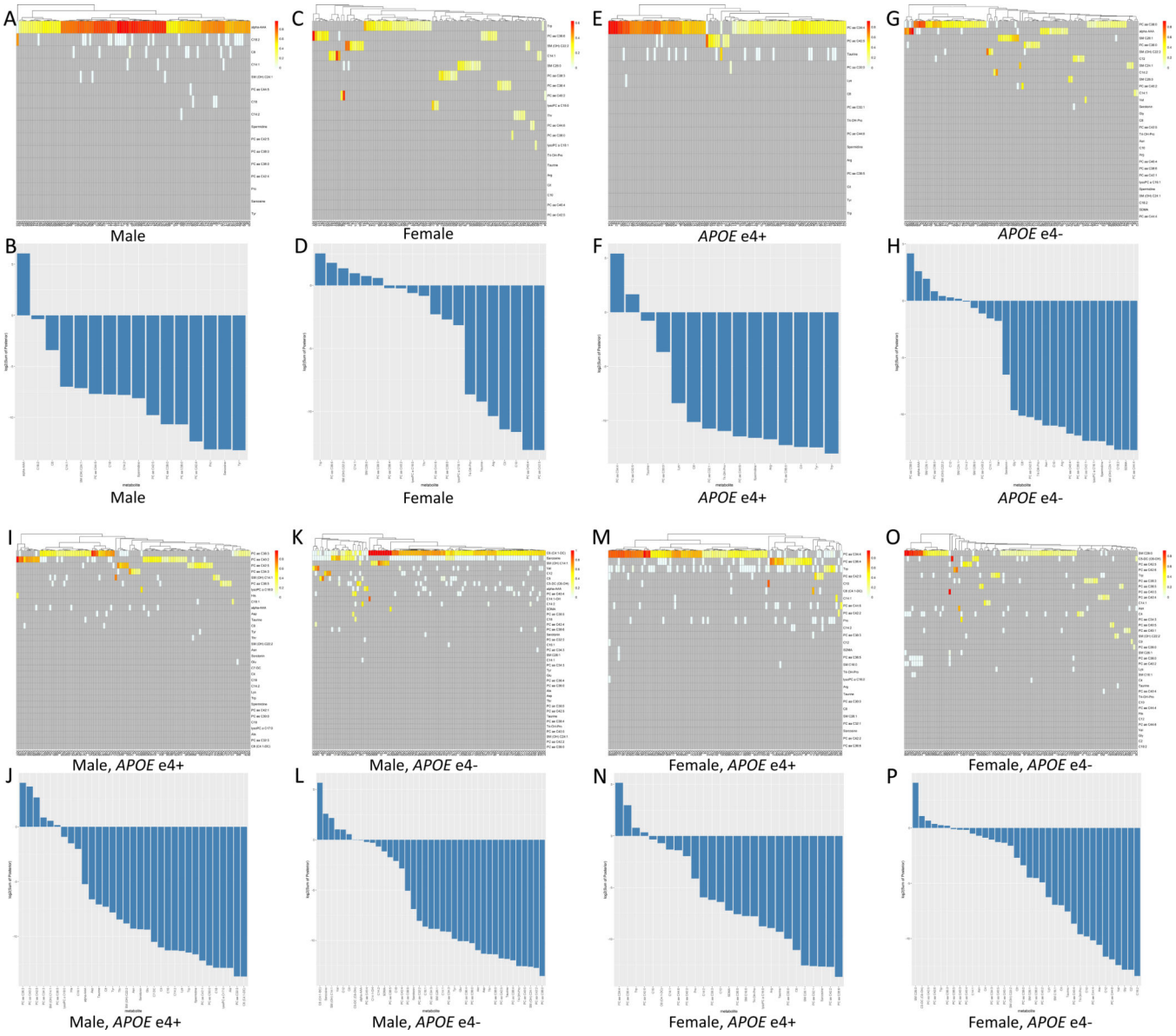

Figure 3. Sex- and *APOE*-specific metabolic heterogeneity

In each group, the confidence and robustness of metabolic drivers were shown in the heatmap where the X-axis represents 100 different networks and Y-axis represents candidate key drivers in 100 networks. Each row in the heatmap represents a vector of 100 posterior probability values of the edge from a key driver to Dx derived from 100 networks, and the bar plot is ranked based on the log2 of the sum of the 100 posterior values per key driver in male (A,B), female (C,D), *APOE*ε4+ (E,F), *APOE*ε4- (G,H), male *APOE*ε4+ (I,J), male *APOE*ε4- (K,L), female *APOE*ε4+ (M,N), female *APOE*ε4- (O,P).

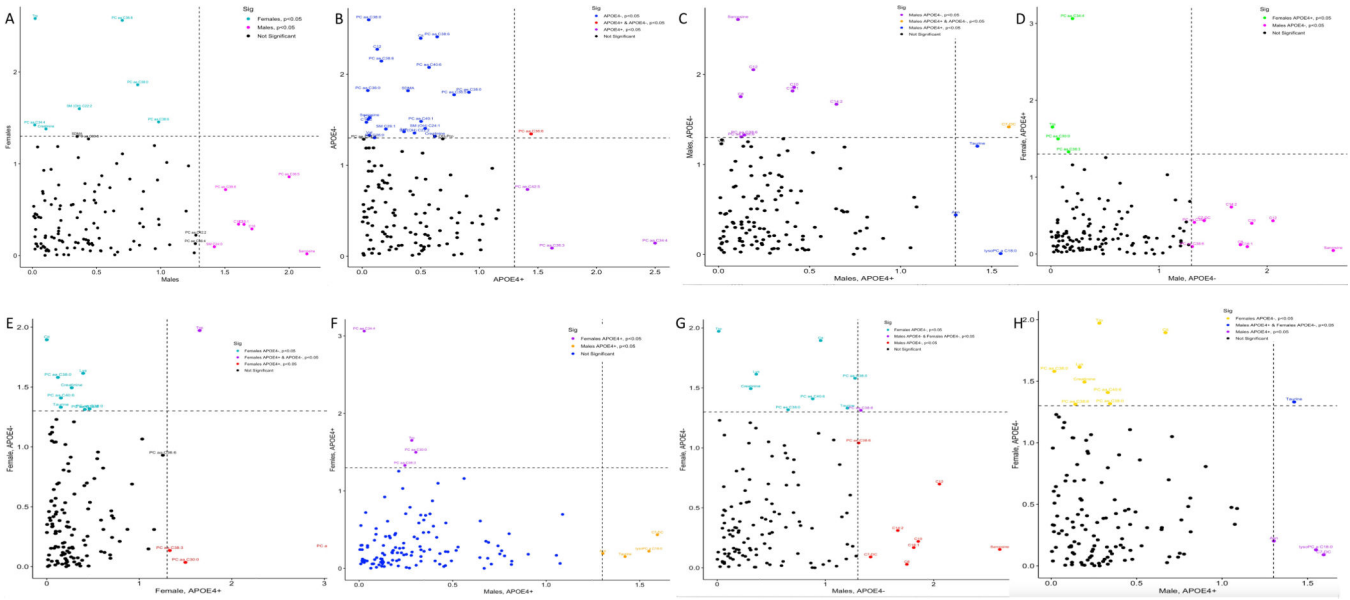

Figure 4. Sex- and *APOE*-specific metabolic differential expression analysis

The significant P-value<0.05 of differentially produced metabolites are compared between patient groups to illustrate the specificity and commonality of AD-associated metabolic signatures to sex and *APOE* genotype. (A) Male *vs* Female; (B) *APOE*ε4+ *vs APOE*ε4-; (C) Male *APOE*ε4+ *vs* Male *APOE*ε4-; (D) Male *APOE*ε4- *vs* Female *APOE*ε4+; (E) Female *APOE*ε4+ *vs* Female *APOE*ε4-; (F) Male *APOE*ε4+ *vs* Female *APOE*ε4+; (G) Male *APOE*ε4- *vs* Female APOEε4+; (H) Male *APOE*ε4+ *vs* Female *APOE*ε4-.

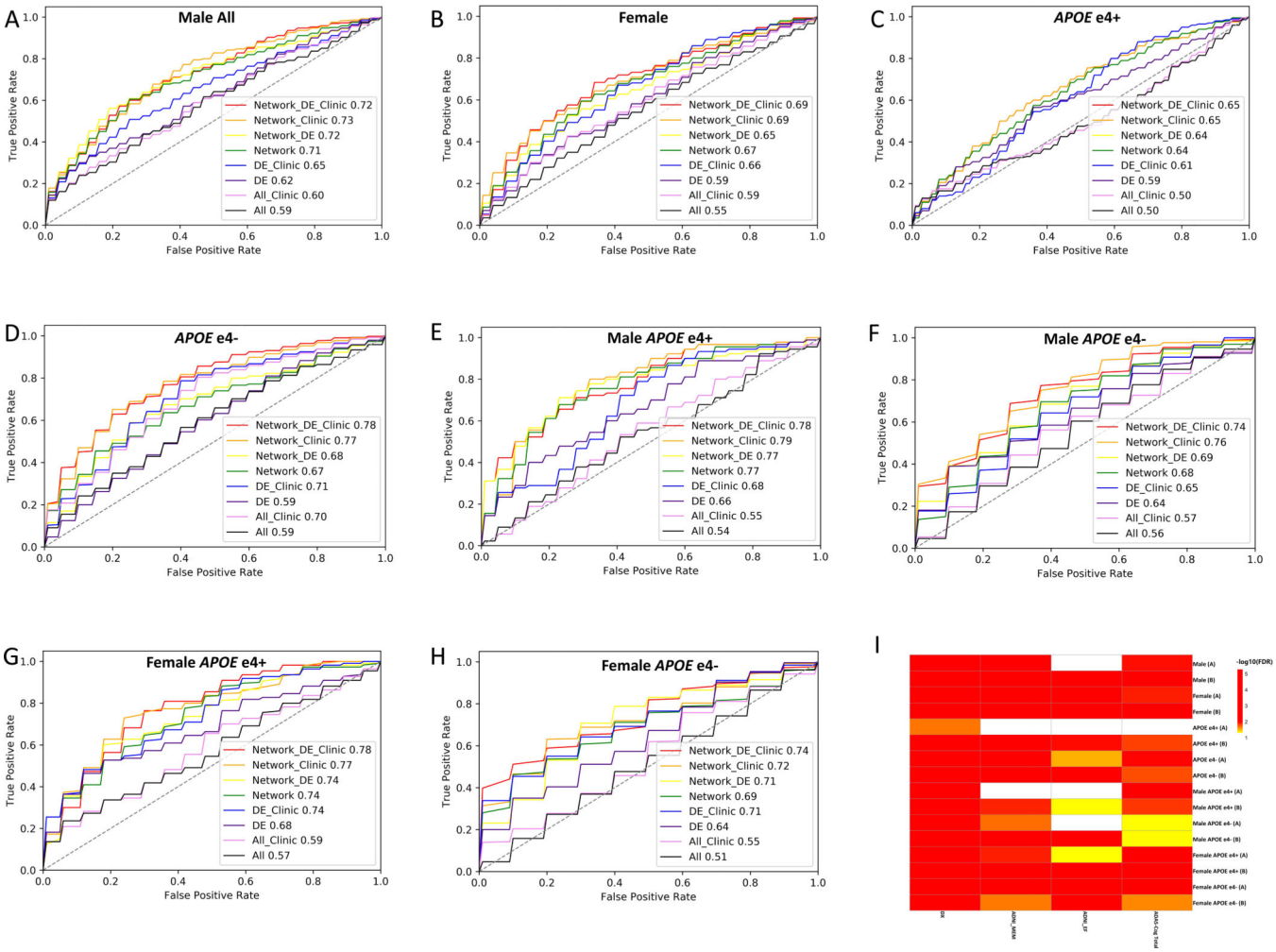

Figure 5. Biomarker panel and cross-validation accuracy for AD diagnosis

The prediction performance of diagnostic biomarker panels derived from different sets of features are compared in each patient group, The number in the figure represents the averaged cross-validation AUC with 8 feature sets respectively in male (A), female (B), *APOE*ε4+ (C), *APOE*ε4- (D), male *APOE*ε4+ (E), male *APOE*ε4- (F), female *APOE*ε4+ (G), male *APOE*ε4- (H); All, all 127 metabolites in the data; All Clinic, all 127 metabolites in the data combines with age, BMI and/or education; DE: significant DE metabolites; DE Clinic: significant DE metabolites combined with age, BMI and/or education; Network: biomarkers derived from metabolic network; Network_DE: biomarkers derived from the combination of significant DE and metabolic network; Network_DE_Clinic: biomarkers derived from combination of significant DE metabolites, metabolic network and age, BMI, and/or education. Network_Clinic: biomarkers derived from metabolic network and age, BMI and/or education; (I) Two selected optimal biomarker panel association with clinical assessment and cognitive decline: The association of the two selected biomarker panel with and without Age, BMI and Education in each patient group (A: biomarker pane derived from metabolic network; B: biomarker pane derived from combination metabolic network plus

age, BMI and/or education) with diagnosis (Dx) and clinical assessments (ADAS-Cog Total Score, memory function (ADNI_MEM) and executive function (ADNI_EF)).

Table 1.

Characteristics of the 1152 ADNI subjects in this study

Demographics	CN	LMCI	AD
Sample size	362	496	294
Sex (M/F)	177/185	307/189	161/133
Age(yr.)	74.61(+/−5.66)	74.11(+/−7.57)	74.71(+/−7.85)
BMI (kg/m^2)	27.04(+/−4.51)	26.49(+/−4.32)	25.87(+/−4.71)
Education(yr.)	16.20(+/−2.79)	15.86(+/−2.91)	15.19(+/−2.99)
***APOE* ε4 +/−**	101/261	265/231	193/101
Clinic Assessment			
ADAS-Cog total score	5.99(+/−3.04)	11.56(+/−4.50)	19.34(+/−6.75)
Memory function (ADNI_MEM)	0.95(+/−0.53)	−0.05(+/−0.57)	−0.73(+/−0.52)
Executive function (ADNI_EF)	0.74(+/−0.70)	0.014(+/−0.78)	−0.82(+/−0.84)
CSF Pathology			
CSF p181-Tau	25.54(+/−14.80)	35.36(+/−17.36)	41.64(+/−19.63)
CSF Aβ1–42	207.67(+/−54.47)	163.48(+/−53.57)	143.64(+/−41.86)

Table 1. Characteristics of the 1152 ADNI participants included in this study

Metabolomics datasets from the Biocrates p180 platform used in the current analyses for the ADNI-1 and ADNI-GO/2 cohorts are available via the Accelerating Medicines Partnership-Alzheimer's Disease (AMP-AD) Knowledge Portal and can be accessed at http://dx.doi.org/10.7303/syn5592519 (ADNI-1) and http://dx.doi.org/10.7303/syn9705278 (ADNI GO-2). The full complement of clinical and demographic data for the ADNI cohorts are hosted on the LONI data sharing platform and can be requested at http://adni.loni.usc.edu/data-samples/access-data/. Abbreviations: ADAS-Cog, Alzheimers Disease Assessment Scale – Cognitive Subscale; BMI, Body Mass Index; CN, cognitively normal; LMCI, Late Mild Cognitive Impairment; AD, Alzheimer's Disease; yr., years. *APOE*ε4−/+: non-carriers and carriers of the *APOE* ε4 allele, ADAS-Cog: Alzheimer's Disease Assessment Scale-Cognitive Subscale, CSF Aβ1–42: Cerebrospinal fluid Amyloid beta 1–42 protein. CSF p181-Tau: Cerebrospinal fluid phosphorylated Tau protein at threonine 181 (p181tau).

Table 2.

Summarize of Sex- and APOE-specific metabolic signature, key drivers and DE metabolites in each patient group.

A. Overall.DE	Overall.KD	Overall Signature
C12↑	PC aa C36:6	PC aa C36:6
C18↑		PC ae C38:0
C18:1↑		PC aa C34:4
C18:2↑		PC ae C40:6
Citruline↑		PC aa C30:0
PC aa C34:4↓		PC aa C38:4
PC aa C36:0↓		
PC aa C36:5↓		
PC aa C36:6↓		
PC aa C38:0↓		
PC aa C38:3↓		
PC aa C38:6↓		
PC aa C40:6↓		
PC aa C42:6↓		
PC ae C36:5↓		
PC ae C38:0↓		
PC ae C38:6↓		
PC ae C40:1↓		
SM (OH) C22:1↓		
SM (OH) C22:2↓		
SM (OH) C24:1↓		

B. Male.DE	Male.KD	Male.Signature
C18↑	alpha-AAA	alpha-AAA
C18:1↑		Val
C18:2↑		Ile
PC ae C36:5↓		Lys
PC ae C38:6↓		Trp
Sarcosine↓		
SM C24:0↓		

C. Female.DE	Female.KD	Female.Signature
Creatinine↑	PC aa C36:6	PC aa C36:6
PC aa C34:4↓	Trp	Trp
PC aa C36:6↓		PC aa C30:0
PC aa C38:6↓		PC ae C38:0
PC ae C38:0↓		PC ae C40:6
SM (OH) C22:2↓		PC aa C34:4
Trp↓		PC aa C36:5

C. Female.DE	Female.KD	Female.Signature
		PC aa C38:6
		Tyr
		C3
		Val
		PC ae C30:0
		PC aa C32:1
		PC aa C32:0
		PC aa C38:0
		PC aa C40:6
		PC ae C40:1
		PC ae C42:3
		PC ae C42:2
		PC aa C42:1
		PC ae C40:5
		PC ae C38:6
		PC aa C34:3
		PC aa C40:4
		PC aa C38:4
		PC aa C38:5
		PC ae C40:4
		Ala
		Asn
		C4
		alpha-AAA
		C0
		Ile
		Lys

D. Male.APOE e4+.DE	Male.APOE e4+.KD	Male.APOE e4+.Signature
Asn↑	PC ae C36:3	PC ae C36:3
C7-DC↓	PC aa C40:2	PC aa C40:2
lysoPC a C18:0↑		PC ae C34:3
Taurine↓		PC ae C34:2
		PC ae C34:1
		SM C16:0
		PC aa C42:2
		PC aa C40:3
		PC ae C32:1
		PC ae C30:0
		PC ae C36:4
		PC ae C36:2
		PC ae C38:3
		PC aa C32:0

D. Male.APOE e4+.DE	Male.APOE e4+.KD	Male.APOE e4+.Signature
		PC ae C34:0
		PC ae C36:1
		PC aa C36:1
		SM C24:1
		SM C24:0
		PC ae C32:2
		PC ae C40:3
		SM C16:1
		SM (OH) C14:1
		PC aa C42:1
		PC ae C42:3
		PC ae C42:1
		PC ae C42:2

E. Female.APOE e4+.DE	Female.APOE e4+.KD	Female.APOE e4+.Signature
PC aa C30:0↓	PC aa C34:4	PC aa C34:4
PC aa C34:4↓	PC ae C36:4	PC ae C36:4
PC aa C38:3↓		PC aa C30:0
Trp↓		PC aa C34:3
		PC aa C36:6
		PC aa C40:4
		PC aa C38:5
		PC ae C34:3
		PC ae C36:5
		PC ae C36:3
		PC ae C38:5
		PC ae C38:4
		PC ae C30:0
		PC aa C32:1
		PC aa C32:0
		PC ae C34:0
		PC ae C38:0
		PC aa C40:6
		PC aa C36:5
		PC aa C38:6
		PC aa C38:3
		PC ae C42:1
		PC ae C40:4
		PC aa C40:5
		PC aa C38:4
		PC ae C40:1
		PC aa C42:5
		PC ae C38:6

E. Female.APOE e4+.DE	Female.APOE e4+.KD	Female.APOE e4+.Signature
		PC ae C32:2
		PC ae C32:1
		PC ae C34:2
		SM C16:0
		PC ae C34:1
		PC aa C40:3
		PC ae C36:2
		PC ae C40:5
		PC ae C44:5
		SM (OH) C16:1
		C18

F. Male.APOE e4-.DE	Male.APOE e4-.KD	Male.APOE e4-.Signature
C10↑	C6 (C4:1-DC)	C6 (C4:1-DC)
C12↑	Sarcosine	Sarcosine
C14:2↑		alpha-AAA
C16:1↑		C8
C7-DC↑		C10
C8↑		C16:1
PC aa C38:6↓		C10:2
PC ae C38:6↓		C5-DC (C6-OH)
Sarcosine↓		C12
		C14:1
		C18:1
		lysoPC a C16:0
		lysoPC a C18:0
		C9
		lysoPC a C17:0
		Glu
		Val
		Ile

G. Female.APOE e4-.DE	Female.APOE e4-.KD	Female.APOE e4-.Signature
Citrulline↑	SM C26:0	SM C26:0
Creatinine↑		SM (OH) C22:1
Lysine↓		SM C26:1
PC aa C38:0↓		SM (OH) C24:1
PC aa C38:6↓		SM C24:0
PC aa C40:6↓		SM (OH) C22:2
PC ae C38:0↓		SM C24:1
Taurine↓		PC ae C40:3
Trp↓		PC ae C40:2
		SM (OH) C16:1

G. Female.APOE e4-.DE	Female.APOE e4-.KD	Female.APOE e4-.Signature
		PC ae C44:5